



CHORUS

This is the accepted manuscript made available via CHORUS. The article has been published as:

Probing Electronic Coherence in a Gas of Dipole-Dipole Coupled Rydberg Atoms

M. R. Kutteruf and R. R. Jones

Phys. Rev. Lett. **108**, 013001 — Published 3 January 2012

DOI: [10.1103/PhysRevLett.108.013001](https://doi.org/10.1103/PhysRevLett.108.013001)

Probing Electronic Coherence in a Gas of Dipole-Dipole Coupled Rydberg Atoms

M.R. Kutteruf and R.R. Jones

Department of Physics, University of Virginia,

Charlottesville, Virginia 22904-4714, USA

Abstract

We demonstrate a novel time-domain method to probe electronic coherence in ensembles of cold Rydberg atoms coupled via nearly resonant dipole-dipole interactions. Short laser pulses create coherent superpositions of few-electron eigenstates which evolve under the influence of pulsed electric fields. The pulses steer the dynamics, enhancing the probability for finding atoms in np , rather than initially excited ns states. The enhancement reflects the underlying electronic coherence which persists for $>10\mu s$, two orders of magnitude longer than previously measured dephasing times in the same system. Simulations suggest that atom motion is responsible for the eventual decoherence.

PACS numbers: 32.80.Ee, 34.20.Cf, 32.80.Qk

Prospects for exploiting dipole-dipole (DD) interactions between Rydberg atoms for quantum information processing [1, 2] have engendered considerable interest in cold Rydberg gases. The generation and manipulation of the few- or many-body entanglement afforded by these interactions is critical for such applications, implicitly demanding local electronic coherence among atoms. In general, coherence does not require uniform coupling between atoms, but inhomogeneities can make characterizing and exploiting it difficult. For example, using rotary echoes, the optical excitation of a cold Rydberg ensemble was found to dephase in $< 1\mu\text{s}$ [3, 4]. Similarly, Ramsey interferometry performed after pulsed laser excitation of DD-coupled atoms established that dephasing times were ~ 100 ns [5]. These results reflect the variation in DD interaction strength throughout an ensemble, but put only a lower limit on the persistence of electronic coherence involving neighboring atoms. While this “microscopic” coherence has been considered theoretically [6–8], to our knowledge it has not been measured.

In this Letter we describe the first measurement of microscopic electronic coherence in cold, DD-coupled Rydberg gases. We employ a time-domain method that is inspired by, but distinct from, spin echo techniques [9]. Short laser pulses excite coherent superpositions of few-electron eigenstates involving neighboring atoms. Due to the DD interaction, these wavepackets evolve from initial configurations in which all Rydberg atoms are in s-states, into those where there is some probability for finding atoms in p-states. Sequences of electric field pulses modify the couplings between atoms and, accordingly, the composition of the constituent few-electron eigenstates. Through the pulse sequence, constructive interference enhances the production of p-state atoms. The decay in this enhancement provides a measure of the multi-electron coherence which persists for $> 10\mu\text{s}$.

Our measurements focus on the evolution of a cold Rb Rydberg gas in the presence of tunable DD-interactions. We begin by considering the electron dynamics of isolated atom pairs before extending the discussion to three or more coupled atoms. Envision two Rydberg atoms, α and β , with eigenstates $|S\rangle$, $|P\rangle$ and $|S'\rangle$, $|P'\rangle$, and transition dipole moments $\mu_\alpha \sim \langle S|r|P\rangle$ and $\mu_\beta \sim \langle S'|r|P'\rangle$, respectively. In the experiments, $|S\rangle$, $|P\rangle$, $|S'\rangle$, and $|P'\rangle$ correspond to $|25s\rangle$, $|24p_{1/2}\rangle$, $|33s\rangle$, and $|34p_{3/2}, |m_j\rangle$, respectively. The energy E of an uncoupled atom pair in $|P\rangle|P'\rangle$, relative to that in $|S\rangle|S'\rangle$, can be Stark tuned through resonance ($E = 0$) using an external electric field [10]. When separated by a distance R , atoms α and β are coupled by a tunable DD interaction $V_0 \sim \mu_\alpha\mu_\beta/R^3$.

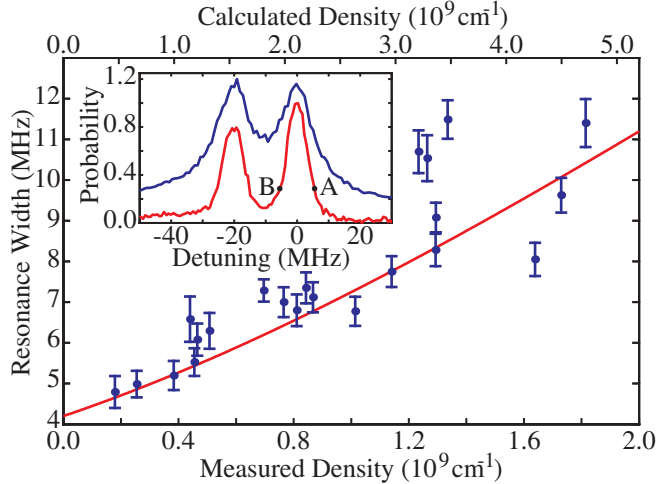


FIG. 1. Inset: Measured transition probability \mathcal{P} as a function of detuning from resonance at calculated densities $\rho = 5 \times 10^9 \text{ cm}^{-3}$ (upper blue) and $\rho = 2 \times 10^9 \text{ cm}^{-3}$ (lower red). The two peaks centered at $F = 3.0$ and $F = 3.4 \text{ V/cm}$ correspond to the $|S\rangle|S'\rangle \leftrightarrow |P\rangle|P'\rangle, |m_j| = 1/2\rangle$ and $|S\rangle|S'\rangle \leftrightarrow |P\rangle|P'\rangle, |m_j| = 3/2\rangle$ resonances, respectively. Near these resonances, E varies approximately linearly vs F with a slope of 51 MHz/(V/cm) [11]. A and B mark the high and low field detunings ($\pm 5.5 \text{ MHz}$) at which the coherence measurements (see Fig. 2) were performed. Main: $|S\rangle|S'\rangle \leftrightarrow |P\rangle|P'\rangle, |m_j| = 3/2\rangle$ resonance width as a function of Rydberg density. The red line shows the predicted width (upper density axis) assuming pure two-body interactions.

Ignoring much weaker, non-resonant van der Waals couplings involving other states, the atom pair has two nearly degenerate eigenstates $|+\rangle = \cos \frac{\theta}{2} |S\rangle|S'\rangle + \sin \frac{\theta}{2} |P\rangle|P'\rangle$ and $|-\rangle = -\sin \frac{\theta}{2} |S\rangle|S'\rangle + \cos \frac{\theta}{2} |P\rangle|P'\rangle$ where $\tan \theta = 2V_0/E$. These eigenstates have energies $\epsilon_{\pm} = (E \pm \gamma)/2$, where $\gamma = \sqrt{E^2 + 4V_0^2}$, and exhibit a standard avoided level crossing as a function of E , with an energy separation $2V_0$ at $E = 0$.

At $t = 0$, $70 \mu\text{K}$ Rb atoms in a magneto-optical trap (MOT) are exposed to two, 5 ns dye laser pulses with wavelengths of 484.1 nm and 481.6 nm . The lasers are tuned to excite atoms from the upper $5p_{3/2}$ trap level to $|S\rangle$ and $|S'\rangle$ in the presence of a weak electric tuning field, $F < 5 \text{ V/cm}$. For narrow band excitation, the level shifts ϵ_{\pm} between DD-coupled atoms, initiating a Rydberg blockade [1]. However, because the $\sim 100 \text{ MHz}$ coherent bandwidths of our 5 ns pulses greatly exceed the Rydberg-pair eigenstate splitting ($2V_0 < 10 \text{ MHz}$, at the Rydberg densities $\rho < 5 \times 10^9 \text{ cm}^{-3}$ used in

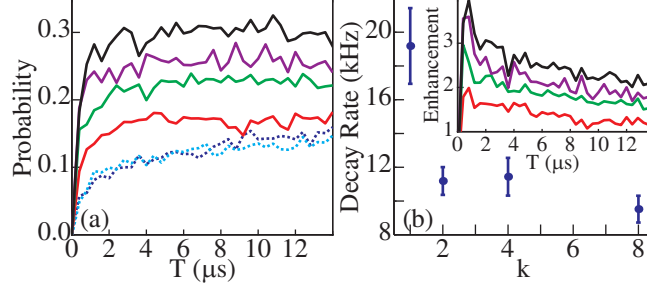


FIG. 2. (a) Measured transition probability as a function of total interaction time, T , for different pulse sequences for $\rho = 2 \times 10^9 \text{ cm}^{-3}$. The solid curves show \mathcal{P}_k for the base sequence $k=1$ (red) and its repetitions, $k=2$ (green), 4(purple), and 8(black). The dashed lines show \mathcal{P}_0 when the atoms are held on the high (dashed blue) or low (dashed cyan) field side of the resonance (A and B in Fig. 1) for the entire time T . (b) Inset: Signal enhancement χ_k vs. T obtained by dividing the solid curves in (a) by the average of the dashed curves. Main: Enhancement decay rate vs. k for the data shown in the inset.

the experiments), we observe no excitation suppression. Instead, isolated pairs are excited to coherent superpositions of $|+\rangle$ and $|-\rangle$ eigenstates. The same electronic coherence that underlies the entanglement established via the Rydberg blockade also defines the dynamics of these two-electron wavepackets. Specifically, since the laser excitation proceeds through the $|S\rangle|S'\rangle$ character of the eigenstates in a time much shorter than $\pi/V_0 \sim 1 \mu\text{s}$, the initial wavefunction for the Rydberg pair is $\Psi(0) = |S\rangle|S'\rangle$. As long as coherence is maintained, this wavefunction evolves according to the Rabi formula:

$$\Psi(t) = (\cos \phi - i\eta \sin \phi)|S\rangle|S'\rangle + i\xi \sin \phi|P\rangle|P'\rangle \quad (1)$$

where $\phi = \gamma t/2$, $\xi = 2V_0/\gamma$, $\eta = E/\gamma$, and γ is the Rabi frequency,.

We use the transfer of population from $|S\rangle|S'\rangle$ to $|P\rangle|P'\rangle$ to characterize both the coupling strength between atoms and the electronic coherence. To this end, state-selective field ionization is employed to measure the probability \mathcal{P} for finding atoms in $|P\rangle$ and $|P'\rangle$ as a function of the detuning E (see Fig. 1) and time T after excitation (see Fig. 2).

Fig.1 shows $\mathcal{P}(E)$ for an interaction time, $T \simeq 2\mu\text{s}$. Two resonances, associated with $|m_j| = 1/2, 3/2$, are visible. Our measurements focus on the DD mediated dynamics near the $|m_j| = 3/2$ resonance, so we define E as the detuning relative to its center. As expected, the resonance lineshapes broaden with increasing ρ due to the decrease in the most probable

distance between nearest neighbor atoms, $R_0 = (2\pi\rho)^{-1/3}$. Fig.1 also shows the $|m_j| = 3/2$ resonance width (FWHM) as a function of ρ . The width increases linearly, exhibiting a minimum width of ~ 4 MHz for $\rho \rightarrow 0$. This non-zero minimum is attributed to electric and magnetic field inhomogeneities in the laser-atom interaction region. The measured widths, including the inhomogeneous contribution, are in good agreement with previous experiments [5].

According to Eq. 1, $\mathcal{P} = \xi^2 \sin^2 \gamma T/2$ at a time T after excitation. The predicted temporal modulations can be interpreted as Rabi oscillations due to the $|S\rangle|S'\rangle \leftrightarrow |P\rangle|P'\rangle$ coupling, or as a quantum beat between different modes in the evolving multi-electron wavepacket. The oscillation amplitude, ξ^2 , is a Lorentzian function of E , representing a resonance with a FWHM, $4V_0$ (see Fig. 1 inset). In the experiment γ and V_0 vary randomly with R for individual atom pairs. Consequently, the resonance lineshape is a cusp rather than a Lorentzian [12]. Moreover, a monotonic increase and saturation, but no oscillations, are observed in $\mathcal{P}(\mathcal{T})$ (see Fig. 2). This does not imply an absence of coherence among individual atom pairs, but instead is a reflection of macroscopic inhomogeneities in R .

The solid curve plotted with the data in Fig. 1 is the result of a calculation that considers only isolated, stationary atom pairs. Ignoring spin, the initial pair state $|S\rangle|S'\rangle$ has zero angular momentum and the tunable DD interaction potential reduces to $V_0 = \sqrt{\frac{2}{3}}\mu_\alpha\mu_\beta/R^3$ with $\mu_\alpha \simeq 490(a.u.)$ and $\mu_B \simeq 128(a.u.)$ [5, 13]. Using Eq. 1 and the nearest neighbor distribution function for a random Rydberg ensemble of density ρ , we compute $\mathcal{P}(E)$ for the ensemble. The solid curve in Fig. 1 is the FWHM of this lineshape, convoluted with an inhomogeneous Gaussian contribution with a 4.2 MHz FWHM. The calculated density at a given resonance width is $\sim 2.6\times$ larger than that determined experimentally. This discrepancy is comparable to the uncertainty in the Rydberg density measurement.

Of course, atoms in the experiment are not isolated in pairs and, in addition to the primary $|S\rangle|S'\rangle \leftrightarrow |P\rangle|P'\rangle$ interactions, DD-couplings mediating coherent exchange or “hopping” processes involving three or more atoms (e.g. $|S\rangle|S'\rangle|P\rangle \leftrightarrow |P\rangle|S'\rangle|S\rangle$, $|P\rangle|P'\rangle|S\rangle \leftrightarrow |P\rangle|S\rangle|P'\rangle$, *etc.*) are also active [11, 14]. These beyond nearest neighbor interactions can influence the system dynamics as well as the energy and delay dependence of our experimental observable, \mathcal{P} . These exchange processes involve degenerate states only in the absence of other position-dependent interactions. Thus, while they cannot be directly controlled via electric field tuning, their common classification as “always resonant” is misleading.

Exchange complicates the electronic eigenstates and dynamics, but does not lead to decoherence among neighboring atoms. Near $E = 0$ the few-electron spectrum is characterized by a large number of nearly degenerate, eigenstates which no longer have the simple form of the $|+\rangle$ and $|-\rangle$ states defined above. Although the dynamics are more complex, following their short pulse excitation the multi-electron wavepackets should still evolve coherently, with a time-dependent transition probability \mathcal{P} that reflects the energy spectrum and composition of the constituent eigenstates.

We consider beyond nearest neighbor interactions by employing a numerical model involving three identical, stationary, spinless S -atoms subject to pairwise couplings V_0 , $V_1 = \frac{4}{9}\mu_A^2/R^3$, and $V_2 = \frac{4}{9}\mu_B^2/R^3$ associated with tunable $SS \leftrightarrow PP'$, and non-tunable $SP \leftrightarrow PS$ and $SP' \leftrightarrow P'S$, interactions, respectively. V_1 and V_2 are the exchange matrix elements averaged over the orientation of the third atom relative to the line connecting the nearest neighbor pair [13]. The Hamiltonian is diagonalized and the initial $|S\rangle|S\rangle|S\rangle$ wavepacket is propagated to a delay T to compute $\mathcal{P}(E)$ for a given set of atom positions. The final lineshape is constructed by integrating the individual $\mathcal{P}(E)$ determinations over the nearest- and next-nearest-neighbor distribution functions for the ensemble. We find that the width of the 3-atom lineshape is only 3% larger than the 2-atom result, but the maximum transition probability is 30% greater. Apparently, exchange influences the dynamics, but the resonance widths are dominated by 2-body, nearest neighbor interactions [7]. This conclusion agrees with that reached through more complete calculations [7, 15] but differs from that drawn from previous experiments [5, 11, 14].

Upon repeating the Ramsey interference measurements of Anderson *et al.* [5], we find dephasing times similar to what they observed and attributed to multi-atom exchange. This dephasing, which does not imply microscopic decoherence, is due to the macroscopic variation in exchange coupling strengths and accrues during times when the primary $|S\rangle|S'\rangle \leftrightarrow |P\rangle|P'\rangle$ interaction is tuned off resonance. On resonance, the energy shifts associated with strong nearest neighbor interactions can partially suppress the exchange coupling to other atoms [7]. An analogous effect, with the tunable DD interaction replaced by an rf field, has been used to preserve Rydberg wavepacket coherence by dynamically decoupling the constituent states from environmental noise [16].

Having characterized the impact and interplay of the tunable and non-tunable interactions on the population transfer, we can investigate the multi-electron coherence of our system. In

particular, we probe the microscopic coherence when atoms are tuned near DD-resonance. Our method is insensitive to inhomogeneities in the dynamics caused by variations in DD-coupling strength at different locations within the ensemble. We employ a series of electric field pulses which modify the DD couplings between atoms, coherently manipulating the composition and energies of the constituent multi-electron eigenstates. The pulse sequence enhances \mathcal{P} at the observation time if, and only if, the system evolves coherently.

For the measurement, atoms are laser excited in a field $F \simeq 3.9$ V/cm, well-detuned from the $|m_j| = 3/2$ resonance. F is then suddenly (~ 2 ns) decreased to the high field wing of the resonance profile (A in the inset of Fig. 1), switching-on the resonant coupling between atoms. After a time $T/2$, the field is reduced again, projecting the system to a point of equal transition probability on the low field side of the resonance (B in Fig. 1). The atoms interact for an additional time $T/2$ before they are again far-detuned to the high field side of the resonance where the final state distribution is measured. Figure 2 shows that this sequence leads to a transition probability, \mathcal{P}_1 , that is substantially greater than the probability \mathcal{P}_0 obtained when the atoms remain on either the high- or low-field side of the resonance for an equivalent net interaction time T . Notably, if this base sequence is repeated k times for $2k$ equal interaction intervals in a total time T , the signal enhancement $\chi_k = \mathcal{P}_k/\mathcal{P}_0$ increases with k . Identical enhancements are observed when the high-to-low field-ordering of the pulse sequences is reversed. However, no enhancement ($\chi_k = 1$) is observed for highly asymmetric time intervals in which, for example, the atoms are left at points A and B for $T - 10$ ns and 10 ns, respectively. Thus, the enhancement is not simply the result of the back and forth traversal of the resonance. In all cases, $\chi_k(T)$ decreases approximately exponentially, approaching unity for large delays.

We can understand the source of the enhancement using the 2-atom model. According to Eq. 1, when the atoms are detuned on one side of resonance, the $|S\rangle|S'\rangle$ amplitude develops an imaginary component proportional to η . This phase advance limits the maximum achievable $|P\rangle|P'\rangle$ probability. Reversing the detuning ($\eta \rightarrow -\eta$) initiates a phase slip that counters the initial advance. The net result is an enhancement in the p-state transition probability. The effect is analogous to enhancement of optical frequency conversion efficiency through quasi-phase-matching in a non-linear crystal. In our case, the phase correction is performed directly in the time domain rather than through a spatial variation of the index of refraction along a laser's path.

By consecutively applying the standard two-level transfer matrix responsible for Eq. 1, with scaled detunings $\eta = \pm\eta_0$ at points A and B, the enhancement factor for the $k = 1$ sequence is easily computed. Assuming microscopic coherence is maintained throughout, $\chi_1 = 1 + \eta_0^2 \tan^2[\gamma T/4]$, for any detuning, atom separation, and net interaction time T . Thus, the signal enhancement survives integration over the distribution of nearest neighbor separations in the MOT. Similar enhancements are predicted by the 3-atom numerical model, indicating that the interference is not fundamentally altered by exchange interactions. The calculated enhancement grows with the detuning, η_0 . Similar increases are observed experimentally. However, p-state excitation via the $|m_j| = 1/2$ resonance (see Fig. 1) limits the maximum density and detuning for which the measurements are straightforward to interpret. For the range of accessible detunings, both models yield $\chi_1 \sim 1.5$ to 2, in good agreement with observations. Provided the total population transfer probability has not saturated near unity, both simulations also predict increases in χ_k with k , comparable to what is seen in the experiment.

As described, the signal enhancement is due to constructive interference between the p-state amplitudes acquired during the temporally separated interaction times. [17] Without this interference, and the coherence that enables it, transporting the system from A to B would have no effect on the net transition probability. The enhancement is observable in spite of the non-uniform atom spacings which lead to variations in the multi-electron dynamics and transition probabilities. Apparently, $\chi_k > 1$ requires microscopic coherence, not identical dynamics throughout the ensemble. Importantly, the decay of χ_k defines the rate at which this coherence is lost. For the data in Fig. 2, this rate is 10-20 kHz, indicating a coherence time of 8-16 μs for $\rho \sim 10^9 cm^{-3}$. [18]

Notably, the loss of coherence reflected by the measured decay in χ_k is not predicted by simulations which assume stationary atoms. In the experiments, atoms move due to their thermal energy and mutual DD forces. For $\rho = 2 \times 10^9 cm^{-3}$, the most probable atom separation is $R \sim 4 \mu m$ and the rms relative velocity between the atoms is $0.2 \mu m/\mu s$. In a $10 \mu s$ interval, the separation between typical nearest neighbors changes by 50% due to their thermal motion alone. This is $4\times$ greater than that expected from DD forces. Because the electronic and center of mass degrees of freedom are coupled by the DD-interaction, relative atom motion introduces an explicit time-dependence in the few-body Hamiltonian which serves as a source of electronic decoherence.

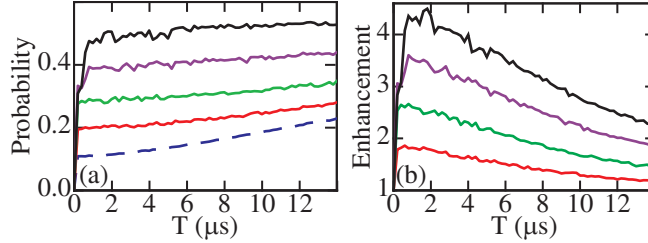


FIG. 3. (a) Transition probabilities and (b) enhancement factors χ_k as a function of the total time on resonance, T , calculated for different pulse sequences using a 3-atom model in which one atom moves. The dashed line shows the average value of \mathcal{P}_0 computed for atoms remaining on the high and low field sides of the resonance. The solid lines show $k = 1$ (red), $k = 2$ (green), $k = 4$ (violet) and $k = 8$ (black).

To model the relative atom motion, we neglect the influence of DD forces but allow one atom in a nearest neighbor pair to move along a line, toward or away from its partner, with a constant speed v chosen at random from within the relative velocity distribution of the ensemble. The 3-atom Hamiltonian is re-diagonalized in sufficiently small time steps to propagate the system through the measurement sequence. Fig. 3 shows the results of the 3-atom calculations for the experimental conditions used to obtain Fig. 2. Despite the crudeness of the model, the simulations are in qualitative agreement with the data. First, both the calculated and measured \mathcal{P}_0 curves *increase* as a function of T . Presumably this increase is due to the broadening of the resonance profile and the concomitant incoherent increase in the transition probability for atom pairs whose separations decrease during the pulse. Second, the pulse sequences yield population transfers that increase more slowly, or are approximately independent of T . Third, the simulated curves show a pronounced decay in χ_k at a rate comparable to that observed in the experiment. This suggests that relative atom motion is a significant contributor to the measured decoherence.

In summary, we have demonstrated a novel time-domain technique to probe microscopic electronic coherence in the presence of resonant DD-interactions in a cold Rydberg gas. We find coherence times that exceed the dephasing times measured using rotary echoes [3, 4] and Ramsey interferometry [5] by one and two orders of magnitude, respectively. Numerical modeling indicates that the coherence is not compromised by beyond nearest neighbor couplings. Rather, atom motion is primarily responsible for the eventual decoherence. Ex-

perimentally there is some evidence that the decoherence rate is reduced when the system is transported across resonance multiple times. The possibility of using pulse sequences to dynamically decouple electronic and center of mass degrees of freedom may be pursued in the future [19].

It is a pleasure to acknowledge helpful conversations with T.F. Gallagher and support from NSF and AFOSR.

-
- [1] D. Jaksch *et al.*, Phys. Rev. Lett., **85**, 2208 (2000); M. D. Lukin *et al.*, *ibid.*, **87**, 037901 (2001).
 - [2] E. Brion, K. Molmer, and M. Saffman, Phys. Rev. Lett., **99**, 260501 (2007); M. Saffman, T. Walker, and K. Molmer, Rev. Mod. Phys., **82**, 2313 (2010).
 - [3] U. Raitzsch *et al.*, Phys. Rev. Lett., **100**, 013002 (2008).
 - [4] K. C. Younge and G. Raithel, N. J. Phys., **11**, 043006 (2009).
 - [5] W. Anderson *et al.*, Phys. Rev. A, **65**, 063404 (2002).
 - [6] S. Westermann *et al.*, Eur. Phys. J. D, **40**, 37 (2006).
 - [7] B. Sun and F. Robicheaux, Phys. Rev. A, **78**, 040701 (2008).
 - [8] J. V. Hernandez and F. Robicheaux, J. Phys. B, **41**, 195301 (2008).
 - [9] C. P. Slichter, *Principles of Magnetic Resonance*, 2nd ed. (Springer-Verlag, 1980).
 - [10] T. F. Gallagher, *Rydberg Atoms* (Cambridge University Press, 1994).
 - [11] W. R. Anderson, J. R. Veale, and T. F. Gallagher, Phys. Rev. Lett., **80**, 249 (1998).
 - [12] M. R. Kutteruf, *Coherence in Rydberg Atoms: Measurement and Control*, Ph.D. thesis, Univ of Virginia (2010).
 - [13] M. R. Kutteruf and R. R. Jones, Phys. Rev. A, **82**, 063409 (2010).
 - [14] I. Mourachko *et al.*, Phys. Rev. Lett., **80**, 253 (1998).
 - [15] K. Younge *et al.*, Phys. Rev. A, **79**, 043420 (2009).
 - [16] R. Minns *et al.*, J. Phys. B, **41**, 074012 (2008).
 - [17] In principle, a signal enhancement with the base sequence ($k = 1$) could be due to local-field shifting of the resonance. Because \mathcal{P}_0 rapidly saturates, if the primary contributions to the signals at A and B come from different sets of atoms, spending a time $T/2$ at both detunings could result in a signal enhancement up to $2\times$. We minimize this effect by working at densities

where the resonance width exceeds the inhomogeneous width, and choosing A and B in the profile wings where the transition probability is dominated by the homogeneous contribution. The increase in enhancement for $k > 1$ cannot be the result of inhomogeneous broadening.

[18] Measurements with $\rho \sim 1 \times 10^9 \text{ cm}^{-3}$ and $\rho \sim 3 \times 10^9 \text{ cm}^{-3}$ show a less pronounced enhancement, likely due to the increased influences of inhomogeneous broadening and the $|m_j| = 1/2$ resonance, but exhibit similar decay rates. This is not surprising given the measurement uncertainties and the fact that the most probable atom separation varies only from $3.8 \mu\text{m}$ to $5.4 \mu\text{m}$ over the densities studied.

[19] R. Minns *et al.*, Phys. Rev. Lett., **97**, 040504 (2006).